J. Membrane Biol. 132, 183–199 (1993)

The Journal of
Membrane Biology

Gating and Conductance in an Outward-Rectifying K^+ Channel from the Plasma Membrane of *Saccharomyces cerevisiae*

Adam Bertl†,*, Clifford L. Slayman†, and Dietrich Gradmann‡

†Department of Cellular and Molecular Physiology, Yale School of Medicine, New Haven, Connecticut 06510 and
‡Pflanzenphysiologisches Institut, Universität Göttingen, 3400 Göttingen, Germany

Summary. The plasma membrane of the yeast *Saccharomyces cerevisiae* has been investigated by patch-clamp techniques, focusing upon the most conspicuous ion channel in that membrane, a K^+-selective channel. In simple observations on inside-out patches, the channel is predominantly closed at negative membrane voltages, but opens upon polarization towards positive voltages, typically displaying long flickery openings of several hundred milliseconds, separated by long *gaps* (*G*). Elevating cytoplasmic calcium shortens the gaps but also introduces brief *blocks* (*B*, closures of 2–3 msec duration). On the assumption that the flickery open intervals constitute bursts of very brief openings and closings, below the time resolution of the recording system, analysis via the beta distribution revealed typical closed durations (*interrupts*, *I*) near 0.3 msec, and similar open durations. Overall behavior of the channel is most simply described by a kinetic model with a single open state (*O*), and three parallel closed states with significantly different lifetimes: long (*G*), short (*B*) and very short (*I*). Detailed kinetic analysis of the three open/closed transitions, particularly with varied membrane voltage and cytoplasmic calcium concentration, yielded the following stability constants for channel closure: $K_I = 3.3 \cdot e^{-zu}$ in which $u = eV_m/kT$ is the reduced membrane voltage, and z is the charge number; $K_G = 1.9 \cdot 10^{-4}([Ca^{2+}] \cdot e^{zu})^{-1}$; and $K_B = 2.7 \cdot 10^3([Ca^{2+}] \cdot e^{zu})^2$. Because of the antagonistic effects of both membrane voltage (V_m) and cytoplasmic calcium concentration ($[Ca^{2+}]_{cyt}$) on channel opening from the *B* state, compared with openings from the *G* state, plots of net open probability (P_o) *vs.* either V_m or $[Ca^{2+}]$ are bell-shaped, approaching unity at low calcium (μM) and high voltage (+150 mV), and approaching 0.25 at high calcium (10 mM) and zero voltage. Current-voltage curves of the open channel are sigmoid *vs.* membrane voltage, saturating at large positive or large negative voltages; but time-averaged currents, along the rising limb of P_o (in the range 0 to +150 mV, for 10 μM $[Ca^{2+}]$) make this channel a strong *outward* rectifier. The overall properties of the channel suggest that it functions in balancing charge movements during secondary active transport in *Saccharomyces*.

Key Words K^+ channels · patch clamp · *Saccharomyces* · outward rectifier · voltage dependence · calcium dependence

* *Present address of corresponding author:* Pflanzenphysiologisches Institut, Universität Göttingen, Untere Karspüle 2 3400 Göttingen, Germany

Introduction

Fungal cells, particularly those of *Neurospora* and *Saccharomyces*, have long served as model cells for biochemical and physiological experiments, having the major advantage that they are readily studied via genetics and molecular biology. Thus, the recent growing interest in function and structure of ion channels, particularly in plant-cell systems, has naturally extended to fungi, for which specific earlier evidence of channel function came from observations of action potentials (Fuller & Pickard, 1976; Slayman, Long & Gradmann, 1976; Caldwell, Van Brunt & Harold, 1986), and from identification of strongly rectifying conductances at the extremes of normal membrane voltage (Blatt, Slayman and Lew, *manuscript in preparation*). The first explicit demonstration of ion channels in fungi was the identification, via patch-clamp experiments, of a K^+ channel in the plasma membrane of *Saccharomyces* (Gustin et al., 1986). That was followed by the description of a (mechano-) stress-sensitive channel in the same membrane (Gustin et al., 1988), by a reported assortment of channel-like currents in bilayers to which yeast membrane vesicles had been fused (Gómez-Lagunas et al., 1989), and by demonstrations of a cation channel in the yeast tonoplast (Wada et al., 1987; Tanifuji et al., 1988; Bertl & Slayman, 1990), multi-state cation channels in *Schizosaccharomyces* plasma membrane (Larsson et al., 1992), and again a stress-sensitive channel in *Uromyces* plasmalemma (Zhou et al., 1991).

Despite the impetus given to channel studies in *Saccharomyces* by recent successes in cloning and sequencing genes that encode for K^+ transport molecules (Gaber, Styles & Fink, 1988; Ko, Buckley & Gaber, 1990; Ko & Gaber, 1991) and in functionally expressing plant K^+ transporters in yeast (Anderson

et al., 1992; Sentenac et al., 1992), patch-clamp experiments on yeast plasma membranes had remained difficult (and therefore rare), at least partly because of the peculiar mechanical properties of this particular membrane.

The principal objectives of this study, then, were (i) to refine the procedures for handling *Saccharomyces* in patch-clamp experiments, to make the organism more generally useful; (ii) to obtain a detailed description of the major channel type in yeast plasma membranes, and thereby, (iii) to provide the basis for structure/function studies to be conducted in yeast on native channels as well as on cloned channels of plant and animal origin; and (iv) to quantify both the gating and the conductance characteristics of the major channel type, so that it can be plausibly modeled in kinetic terms.

Materials and Methods

Growth and Handling of Cells

All experiments were carried out on the tetraploid strain YCC78, of *Saccharomyces cerevisiae*, which was selected for its large size (about 1.6× diameter of normal haploid yeast) and was supplied by Dr. Michael Snyder (Yale Department of Biology). The strain, which requires adenine and uracil supplementation, was grown overnight in YPD medium (30 ml per 125-ml Erlenmeyer flask; 25 °C) with rotary shaking at 120 rpm. Cells were harvested by low-speed centrifugation (500 × *g* for 5 min), resuspended in 10 ml buffer A (50 mM KH_2PO_4 titrated to pH 7.2 with KOH, plus 40 mM β-mercaptoethanol) repelleted, resuspended in 3 ml buffer A, and then incubated at 30 °C for 30 min with occasional shaking.

Protoplasts were formed by adding 3 ml of buffer B (50 mM KH_2PO_4 titrated to pH 7.2 with KOH, plus 40 mM β-mercaptoethanol and 2.4 M sorbitol), along with 2 mg/ml zymolyase, 2 mg/ml glucuronidase, and 30 mg/ml BSA. The mixture was then incubated at 30 °C for 45 min, and protoplasts were harvested by low-speed centrifugation and resuspended in buffer C (250 mM KCl, 10 mM $CaCl_2$, 5 mM $MgCl_2$, and 5 mM MES titrated to pH 7.2 with Tris base). This suspension was pelleted, resuspended in buffer C containing 1% glucose. The size of freshly liberated protoplasts varied in the range of 4–6 μm in diameter, with the central vacuole occupying 15–25% of the cell volume.

Seal Formation and Patch Isolation

Larger protoplasts, which are more convenient to work with, were obtained by incubating freshly liberated protoplasts in glucose-supplemented saline (buffer C) at room temperature. This allowed the protoplasts to enlarge without either budding and dividing or regenerating cell walls, and yielded protoplasts up to 15 μm in diameter after 24 hr (Bertl, Gradmann & Slayman, 1992*a*; Bertl & Slayman, 1993). However, highest success rate and easiest seal formation were obtained from protoplasts incubated for about 1–2 hr. Seal formation is aided by high concentrations of $CaCl_2$ (10 mM) and proper osmolality of the bath solution (Spalding et al., 1992), where protoplasts are swollen but safely short of their bursting point. With this procedure, seals of >10 GΩ formed in >50% of the attempts. After seal formation, the high Ca^{2+} bath solution was exchanged by a low (1 μM) Ca^{2+} solution, and inside-out patches were produced by an abrupt and drastically increased perfusion velocity. Low Ca^{2+} in the bath solutions prevents resealing of the membrane and formation of a vesicle within the pipette tip.

Electrical Experiments and Data Acquisition

The actual experiments were carried out using standard patch-clamp techniques (Hamill et al., 1981); and data acquisition and storage were managed with the apparatus described by Bertl and Slayman (1990). Most data were obtained by recording in the inside-out patch configuration. Recording solutions (bath, cytoplasmic side) typically contained 200 mM KCl, 5 mM MES titrated to pH 7.0 with Tris base, plus Ca^{2+}, which was unbuffered at about 100 μM or above and buffered with EGTA at 10 μM or below. Free Ca^{2+} was calculated using a standard computer program (CAMG, 1989, by W.H. Martin, Yale University). Pipette solutions (extracellular side) contained 50 mM KCl, 0.1 mM $CaCl_2$, 250 mM sorbitol, pH 5.5–5.7 unbuffered. The original data (recorded at 20 kHz sampling rate, through a 10-kHz low-pass filter [f_1]) were played back to the computer, usually with lower sampling rates and filter frequencies (f_2). After such serial filtering, the effective frequency was taken as $f = (1/f_1^2 + 1/f_2^2)^{-0.5}$, corresponding to a first-order filter time constant of $\tau = 1/(2\pi f)$. Empirical calibration of the recording system, including the output filter (eight-pole Bessel filter, at frequency f_b) yielded an effective system time-constant, $\tau_r = 0.224/f_b$.

Nomenclature

The kinetic behavior of channels is sufficiently described by an ensemble of open and closed states, along with their specific mean lifetimes, but it is useful also to have an interpretive verbal description for easily observed events. In keeping with conventions already adopted to describe K^+ channels in nerve and muscle membranes (*see* Latorre & Miller, 1983; Hille, 1984; Yellen, 1987), we will use the terms italicized below. When the apparent open state is found to be noisy (*see* Fig. 1*A* and *B*) due to unresolved on/off switching, the enlarged open channel fluctuations (usually asymmetric) will be called *flicker;* the apparent open state will be termed a *burst,* and the long, quiet, closed intervals separating bursts will be named *gaps*. The fast, incompletely resolved closures within bursts will be referred to as *interrupts*. Finally, discrete brief closures, resulting from high positive membrane voltages (V_m) and high cytoplasmic [Ca^{2+}] (*see* Fig. 1*C* and *D*), will be called *blocks*.

Beta Distribution Analysis of Channel Flicker

Although for most purposes, commercial software (pCLAMP, Axon Instruments, Foster City, CA) was used to manage and analyze these experiments, analysis of the flicker data required our own algorithm, which was written to encode the beta distribution function, as described by Yellen (1984). Briefly, channel flicker was assumed to consist of unresolved transitions between

two discrete conductance states: one open state (1) and one closed state (O). If the mean lifetimes of the open state ($\tau_1 = 1/k_{1O}$) and the closed state ($\tau_O = 1/k_{O1}$) of this simple on/off system are shorter than half the effective filter time constant τ_r, the probability density function ($y(x)$) of the observed open-channel amplitude (x, $0 \leq x \leq 1$), expressed as a fraction of the "true" open-channel amplitude, is

$$y(x) = \frac{x^{(a-1)}(1-x)^{(b-1)}}{B(a,b)}, \text{ where } a = \frac{\tau_r}{\tau_O} \text{ and } b = \frac{\tau_r}{\tau_1}, \quad (1)$$

in which τ_r, τ_O, and τ_1 are defined above, and $B(a,b)$ is the beta distribution function, equal to unity when integrated over all amplitudes. The "true" open-channel amplitude (I_O, the denominator of x) is also an intrinsic parameter of Eq. (1).

Practical application of Eq. (1) required correction for intrinsic Gaussian recording noise, seen in the baseline. This was accomplished by accumulating the baseline and burst amplitudes in separate files. Baseline noise was determined as a Gaussian standard deviation, SD_O, and Eq. (1) was numerically convoluted with this Gaussian noise. τ_O, τ_1, and I_o were determined by least-squares fitting of this broadened beta distribution to the experimental data. When τ_O or τ_1 turned out not to be $<\tau_r/2$, the data were refiltered until this requirement was fulfilled (Yellen, 1984).

Kinetic Modeling of Open-Channel Currents

Our enzyme-kinetic description of the channel is based on a unified cyclic model (Läuger, 1980). For practical application, this can be simplified to a two-state model, which was first applied to ion pumps (Hansen et al., 1981) and later to channels as well (Bertl & Gradmann, 1987; Gradmann, Klieber & Hansen, 1987; Bertl, Klieber & Gradmann, 1988; Bertl, 1989; Draber, Schultze & Hansen, 1991; Spalding et al., 1992; Klieber & Gradmann, 1993;). In this model, one pair of apparent rate constants (k_{io} and k_{oi}) stands for a voltage-dependent, reversible transfer of charge (here $z = 1$) between inside (i) and outside (o): $k_{io} = k^0_{io} \cdot e^{zu/2}$ and $k_{io} = k^0_{oi} \cdot e^{-zu/2}$, where the superior 0 denotes the particular value at zero voltage, u is the reduced voltage ($u = V_m e/kT$), e, k and T have their usual thermodynamic meanings, and the factor 2 reflects the assumption of a symmetric Eyring barrier. A second pair of apparent rate constants (κ_{io}, κ_{oi}) represents the remaining, voltage-independent part of the reaction cycle, with all constituent steps lumped together. The overall current-voltage relationship of this model, then, is described by:

$$I_o = ze\frac{k_{io}\kappa_{oi} - k_{oi}\kappa_{io}}{k_{io} + k_{oi} + \kappa_{io} + \kappa_{oi}}. \quad (2)$$

Conventions and Definitions

We use the standard sign convention in electrophysiology (Bertl et al., 1992*b*); transmembrane voltage, V_m, is taken as the electric potential of the cytoplasm minus that of the extracytoplasmic space. Positive charges *leaving* the cytoplasm are designated as *positive* (outward) currents, and are plotted upward in all graphs. Positive charges *entering* the cytoplasm are designated as *negative* (inward) currents, and are plotted downward. An "outward rectifier" has a preferentially high conductance for outward currents, and a low conductance for inward currents.

For an abbreviated presentation of the important information about compositions of media on the two sides of the membrane we use the form {inside/outside}: {200 K, 0.1 Ca/50 K}, for example, means that solution on the cytoplasmic side contained 200 mM K^+ plus 0.1 mM Ca^{2+} and the extracellular solution contained 50 mM K^+. Constant constituents (i.e., [Cl^-], pH, and extracellular [Ca^{2+}]) are usually not specified *in the text,* since their effects were small or unknown, but are listed in general solution compositions (*see* Growth and Handling of Cells, above) and/or in the figure legends.

Results

Basic Description of Channel Behavior

Although occasional patch records from the plasma membrane of *S. cerevisiae* hint at other kinds of channels in that membrane, by far the easiest to observe under our experimental conditions is a potassium selective channel of ~20 pS conductance, in cell-attached patches with 200 mM KCl and 10 mM $CaCl_2$ in the patch pipette. This channel is clearly the same as that first reported by Gustin et al. (1986), and its selectivity for K^+ over other cations, especially Na^+, can readily be demonstrated by substitution experiments in which K^+ removal progressively diminishes the open-channel current to zero. A detailed description of the *selectivity* and *pharmacology* of this channel will be the subject of a separate study.

The main conducting and switching characteristics of this yeast K^+ channel can all be recognized in the recordings shown in Fig. 1. Panel *A* is a set of single-channel records made in the cell-attached mode, illustrating four properties which distinguish this channel from the other well-characterized yeast membrane channel, the tonoplast cation channel (Bertl & Slayman, 1990). The most obvious difference, already referred to above, is the small conductance (G_O) of the open channel: approximately 20 pS in {Cytoplasmic K^+/200 KCl}, calculated from the open-channel current (~3 pA) at a clamped membrane voltage (V_m) of 140 mV. Under comparable conditions, the tonoplast cation channel has a much higher conductance, 120–150 pS.

A second difference is that opening of the plasma membrane channel, which was rarely observed at negative membrane voltages, was enhanced by large positive voltages, i.e., by reverse polarization. Thus, Fig. 1*A* shows increasing channel open probability as voltages go more positive between +60 and +180 mV. [Since the intracellular K^+ concentration in *Saccharomyces* is normally near 150 mM (Jones et al., 1965; Camancho et al.,

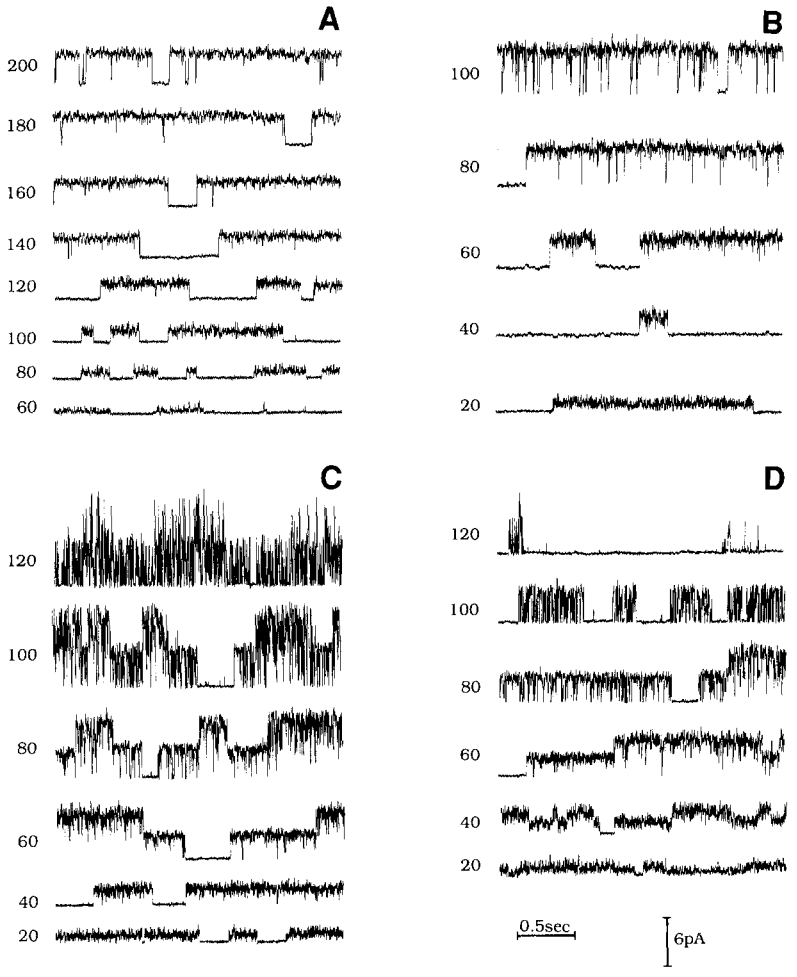

Fig. 1. Survey of gating properties of the major K^+ channel in the plasma membrane of *Saccharomyces*. Current records from a cell-attached patch (*A*), and isolated inside-out patches (*B–D*). Clamped membrane voltage (left of each trace) is stated as cytoplasmic surface (bath) minus external surface (pipette), and here is always positive. The isolated patches were exposed to different free Ca^{2+} concentrations: *B*, 10 μM; *C*, 100 μM; and *D*, 1 mM. Recording solutions: Pipette: 200 mM KCl, 10 mM Ca^{2+}, pH 7 (*A*) or 50 mM KCl + 100 μM $CaCl_2$ equilibrated with air (pH. 5.7–5.9; *B–D*); Bath: 200 mM KCl plus 5 mM MES titrated to pH 7.0 with Tris, plus Ca^{2+} as given above. Bath solution was "cytoplasmic" for the isolated patches. Baseline (current with zero open channels) is at the bottom of each trace. Data low-pass filtered at 200 Hz and sampled at 2 kHz.

Note especially the characteristic increase in current fluctuations during channel-open periods (*see* lower 2–3 traces in each set). Also, the brief full closures at 10 μM Ca^{2+} (*B*) and 80–100 mV, which were dominant at 100 μM Ca^{2+} (*C*) and coalesced to long closed periods at 1 mM Ca^{2+} (*D*).

1981), compared with 200 mM in the patch pipette, the clamp voltage noted to the left of each record should have been within a few mV of the actual membrane voltage.] Two further features are that at moderate positive voltages, the channel tended to be either open or closed for long periods of time (several hundred msec), and that the open-channel currents showed much larger fluctuations than did the baseline. These fluctuations (channel *flicker*) were larger at moderate positive voltages (80–100 mV in Fig. 1*A*) than at higher ones (>120 mV).

The remaining panels of Fig. 1, which represent measurements on isolated membrane patches in the inside-out configuration, confirm these properties and add several new ones. The three sets of records differ only in the concentration of free calcium applied to the cytoplasmic side of the membrane (bath solution): 10 μM in *B*, 100 μM in *C*, and 1 mM in *D*. The traces at low positive voltages (+20 mV, +40 mV, with all three Ca^{2+} concentrations) for the isolated patches demonstrate selectivity of the channel for K^+ over Cl^-, since open-channel currents were always positive. With {200 KCl/50 KCl}, the equilibrium voltage for potassium (E_{K^+}) was near −29 mV, but that for chloride was near +29 mV (equilibrium voltages corrected for activities), and a Cl^--selective channel would have displayed *negative* open-channel currents at +20 mV, and essentially zero current at +30 mV.

Elevating Ca^{2+} on the cytoplasmic side had two very clear effects on channel properties. At low positive voltages, it increased the probability of the channel to be in the flickery open state. And at moderate or large voltages, high $[Ca^{2+}]$ increased the *frequency* of discrete brief closures: these were sparse at the largest voltages with cell-attached patches (Fig. 1*A*), convincing at +80 and +100 mV in 10 μM Ca^{2+}, dominant at the higher voltages in 100 μM Ca^{2+}, and evidently coalesced into long uninterrupted closures at the highest $[Ca^{2+}]_{cyt}$ and voltage (+120 mV in Fig. 1*D*).

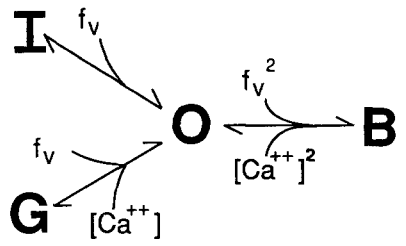

Closed State	Rate Constants	Stability Const.
Interrupt	$O \underset{k_{IO}}{\overset{k_{OI}}{\rightleftharpoons}} I$	$K_I = k_{OI}/k_{IO}$
Block	$O \underset{k_{BO}}{\overset{k_{OB}}{\rightleftharpoons}} B$	$K_B = k_{OB}/k_{BO}$
Gap	$O \underset{k_{GO}}{\overset{k_{OG}}{\rightleftharpoons}} G$	$K_G = k_{OG}/k_{GO}$

Fig. 2. Reaction model to describe the gating properties shown in Fig. 1: three closed states, arranged as parallel transitions from a single open state (O). Closed state I (interrupt) represents very brief closures (sub-millisecond) which were not resolved, but generated flicker in the open-channel traces; state G (gap) represents long closures (the quiet baselines); and state B (block) represents brief calcium-induced closures. At least three of the six implied rate constants (*see table*, bottom panel) are voltage sensitive, as indicated by the reaction factor f_v, which is the Boltzmann term $\exp(zeV_m/kT)$; and at least two are calcium sensitive, as indicated by the concentration term $[Ca^{2+}]$.

A Kinetic Model

From inspection of the original data in Fig. 1, a simple (minimal) model can be derived to represent the switching behavior of the yeast plasma membrane K^+ channel. As shown in Fig. 2, this model consists of a single open state (O) and three independent, parallel, closed states: *gap* (G), referring to the long closed-channel intervals conspicuous at low positive voltages and low Ca^{2+} concentrations (Fig. 1*A,B*); *block* (B), for the discrete brief closures at high positive voltages and high Ca^{2+} (Fig. 1*B,C,D*); and *interrupt* (I), for the brief, incompletely resolved closures within a burst (all panels of Fig. 1). The effects of membrane voltage and calcium concentration are also indicated in Fig. 2, in the form of pseudoreactants, $f_v(= e^{zu})$ and $[Ca^{2+}]$, which push channel opening or closure as noted above. The kinetic order of those effects (one, for transitions $I \rightarrow O$ and $G \rightarrow O$; two for $O \rightarrow B$) is a qualitative aspect which will be derived below.

Quantitative Treatment of the Burst Intervals

Unresolved interrupts should have two easily observable effects on the apparent open-channel current amplitude: asymmetrically broadened channel flicker, already noted, and reduction of the open-channel current due to time averaging. With certain assumptions, these two effects can be analyzed via a beta probability function to yield average parameters for the discrete events. These assumptions are here (i) that the channel displays only one open state (O), with a fixed conductance; (ii) that it has only one closed state (I, for interrupt), here *specifically during the burst intervals*, and (iii) that the overall filter frequency is sufficiently low: in practice, less than half the intrinsic frequency of the opening/closing events (*see* Materials and Methods).

After τ_r was calculated from the filter settings, the fitting procedure yielded values for mean interrupt time (τ_I), mean open time (τ_O), and true open-channel current (I_O). One set of results is illustrated in Fig. 3, for data accumulated at +20, +40, and +60 mV (top to bottom, respectively) from an isolated patch. The current records in the left column of Fig. 3 (point plots, filtered at 2 kHz and sampled at 5 kHz) show an asymmetry which is not obvious in the filled records of Fig. 1. At +20 mV, for example, the density of points is high near the baseline and thins toward more positive currents. This density distribution is reflected in the shape of the corresponding histogram in the right column of Fig. 3, by the tail toward larger currents. For the +60 mV data the situation is reversed, with the point density thinning and the histogram tail stretching toward less positive currents (baseline). The three tics along each current axis indicate the closed-channel current (O), the mean open-channel current (I_m), and the fitted true open-channel current (I_o). The fractional separation between true current and mean current diminished with increasing positive voltage, implying a voltage-dependent increase of open probability ($'P_O$) within the bursts. This is represented in Fig. 2 by entry of f_V on the I–O limb.

The data in Fig. 3 are examples from an experiment with 100 μM Ca^{2+}, but essentially the same results were obtained at all calcium concentrations from 10 μM to 1 mM, demonstrating that the distribution of interrupts, and open probability within a burst, were voltage dependent, but calcium *in*dependent. Plots of τ_I and τ_O *vs.* membrane voltage are shown in Fig. 4, where the differently shaped symbols designate the different Ca^{2+} concentrations tested. Independent regression lines fitted to these log-linear plots (*see* legends to Fig. 4) have slopes of 0.71 per 58.5 mV for τ_O and −0.29 per 58.5 mV

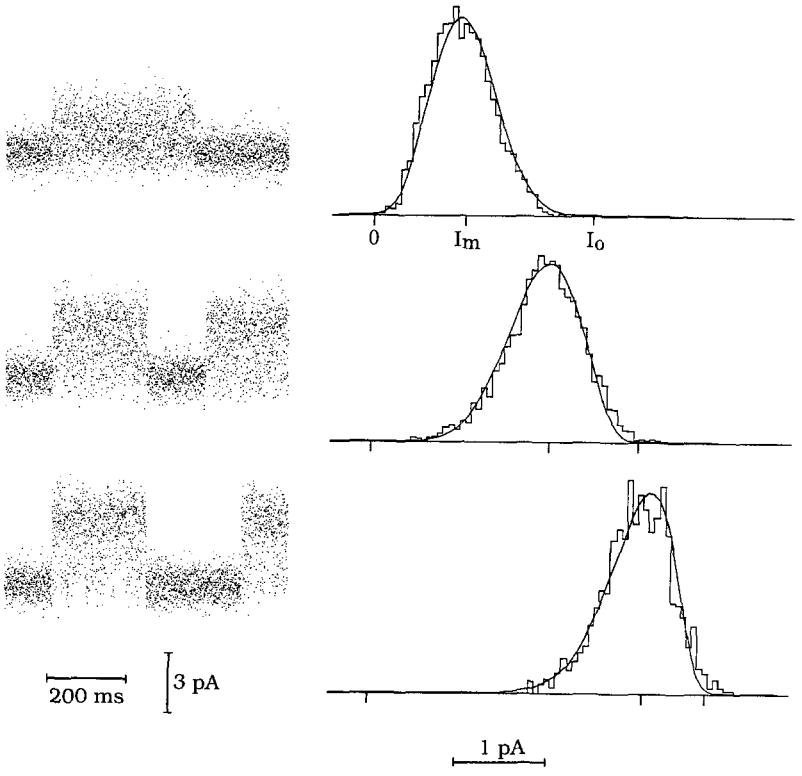

Fig. 3. Examples of beta distribution analysis of flicker in open-channel current data, at three membrane voltages: +20 mV (top), 40 mV (middle), and 60 mV (bottom). Left column: point plots of 800-msec segments of current records, filtered at 2 kHz and sampled at 5 kHz. Right column: Histograms of similar data (longer segments), refiltered at ~100 Hz; fitted beta distributions (text Eq. 1) are superimposed. Baseline serifs (L → R, respectively): zero current (0), mean current (I_m), "true" open-channel current (I_o). All data were taken from Fig. 1*C*, but only flickery open-channel intervals are included in the histograms.

for τ_I, assuming $z = 1$. Interestingly, these numbers render the apparent charge number for voltage gating in this reaction step to be exactly 1.0. The corresponding intercepts at $V_m = 0$ are 0.58 msec and 0.17 msec, and the implied exponential representations of voltage dependence are as follows:

$$\tau_I = 0.58e^{-0.29zu} \text{ and } \tau_O = 0.17e^{0.71zu}, \text{ in msec,} \quad (3)$$

where the voltage coefficients 0.71 and 0.29 locate the peak in an Eyring barrier as a fraction of membrane thickness (or distance between the electric potentials on the two sides of the membrane).

The meaning of these results can perhaps be seen better by reference to the table in Fig. 2. The mean lifetime of the open state within a burst (τ_O) is the reciprocal of the probability for the spontaneous transition $O \rightarrow I$ within a given time interval: $\tau_O = 1/k_{OI}$; and correspondingly, $\tau_I = 1/k_{IO}$ holds for the mean lifetime of the interrupt state. Then the stability constant for interrupt, which is just the ratio of transition probabilities, as given in Fig. 2, is

$$K_I = \frac{k_{OI}}{k_{IO}} = \frac{\tau_I}{\tau_O} \approx 3.3e^{-zu} = K_I^0 e^{-zu}, \quad (4)$$

in which K_I^0 is the I-state stability constant with $V_m = 0$. The open probability ($'P_O$) within the bursts follows simply as

$$'P_O = \frac{\tau_O}{\tau_O + \tau_I} = \frac{1}{1 + K_I} \approx \frac{1}{1 + 3.3e^{-zu}}, \quad (5a)$$

which equals 0.5 with $\tau_O = \tau_I$ at approximately 30 mV in Fig. 4. Finally, the interrupt (closed) probability ($'P_I$) within the bursts is

$$'P_I = \frac{\tau_I}{\tau_O + \tau_I} = \frac{K_I}{1 + K_I} \approx \frac{1}{1 + 3.3e^{zu}}, \quad (5b)$$

Quantitative Treatment of Gaps and Blocks

The channel-open and -closed probabilties, $'P_I$ and $'P_O$, calculated above are *conditional* probabilities; i.e., they depend upon the assumption that the channel be not in the gap or blocked (*G*- or *B*-closed) states. In order to convert these conditional probabilities to the corresponding global probabilities, P_O and P_I, it is necessary to multiply by the joint probability (P_{O+I}) of the open and interrupt states with respect to all time. We call that the burst probability, which is

$$P_{O+I} = \frac{1 + K_I}{1 + K_I + K_G + K_B}, \quad (6)$$

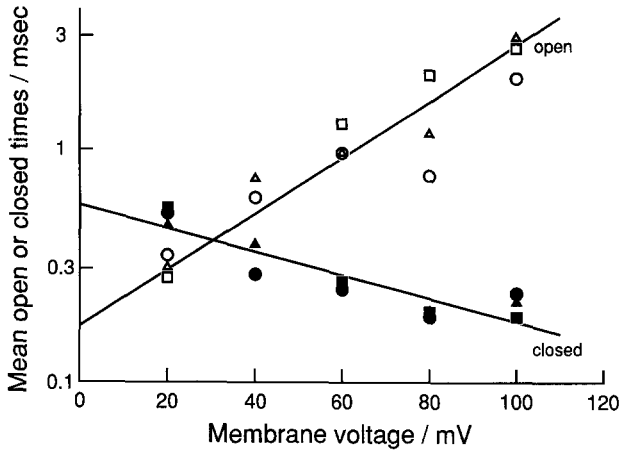

Fig. 4. Voltage dependence, and calcium *in*dependence, of mean residence times (τ_O, τ_I) for the yeast K^+ channel in open and closed states during bursts. Summary results from all experiments similar to those in Fig. 1*B–D*, analyzed by means of the beta distribution, as in Fig. 3. Different symbols designate different Ca^{2+} concentrations in the bath (cytoplasmic) solution: ●, ○ = 10 μM; ■, □ = 100 μM; and ▲, △ = 1 mM.

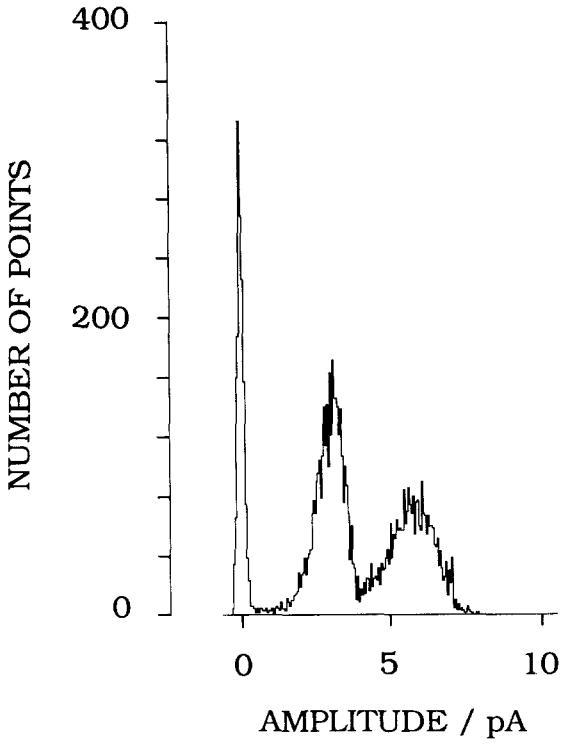

Fig. 5. Typical current-amplitude histogram for a two-channel patch. Data from an extended record with membrane voltage clamped at +60 mV, and solutions as in Fig. 1*C* (100 μM Ca^{2+}). The "open" state represented by such histograms includes the true open state (*O*) plus unresolved interrupts (*I*), so that the areas enclosed by the several peaks can be used to calculate the channel burst probability, P_{O+I}, by means of text Eq. (8).

and the resultant expressions for global probabilities are:

$$P_I = {}'P_I \cdot P_{O+I} = \frac{K_I}{1 + K_I + K_G + K_B} \tag{7a}$$

and

$$P_O = {}'P_O \cdot P_{O+I} = \frac{1}{1 + K_I + K_G + K_B}. \tag{7b}$$

Thus, in order to determine P_O and P_I, a value for $[K_G + K_B]$ is needed.

This can be obtained by noting that P_{O+I} can be separately evaluated from amplitude histograms for multichannel patches containing known numbers of channels. Such a histogram is shown in Fig. 5 for a record taken from the experiment of Fig. 1*C*, with a two-channel patch. The individual peaks in the histograms are broadened and skewed slightly by unresolved interrupts, but the relative areas nevertheless define P_{O+I} as follows:

$$P_{O+I} = \frac{\sum_{i=O}^{n} iA_i}{n \sum_{i=O}^{n} A_i}, \tag{8}$$

in which n is the number of channels in the patch, and A_i is the area under the histogram representing i open channels. Resulting plots of the global P_O *vs.* membrane voltage, for the four conditions in Fig. 1, are shown in Fig. 6. These plots quantify a salient feature in Fig. 1, *viz.*, that the open probability increases with increasingly positive membrane voltages at low Ca^{2+} concentrations (10 μM in Fig. 1*B*; 0.7 μM ≈ $[Ca^{2+}]_{cyt}$ to fit the curve in Fig. 1*A*), but peaks and then decreases with rising positive membrane voltages at higher $[Ca^{2+}]_{cyt}$. Combining Eqs. (6) and (8) yields

$$K_G + K_B = \frac{1 - P_{O+I}}{P_{O+I}}(1 + K_I) = \frac{\sum_{i=O}^{n} (n - i)A_i}{\sum_{i=O}^{n} iA_i}(1 + K_I). \tag{9}$$

The *plots* of Fig. 6 clearly show that $[Ca^{2+}]_{cyt}$ and V_m dependencies of open probability with respect to the gap state to differ from those with respect to the blocked state. That means that if a form for these dependencies is assigned, then the associated pa-

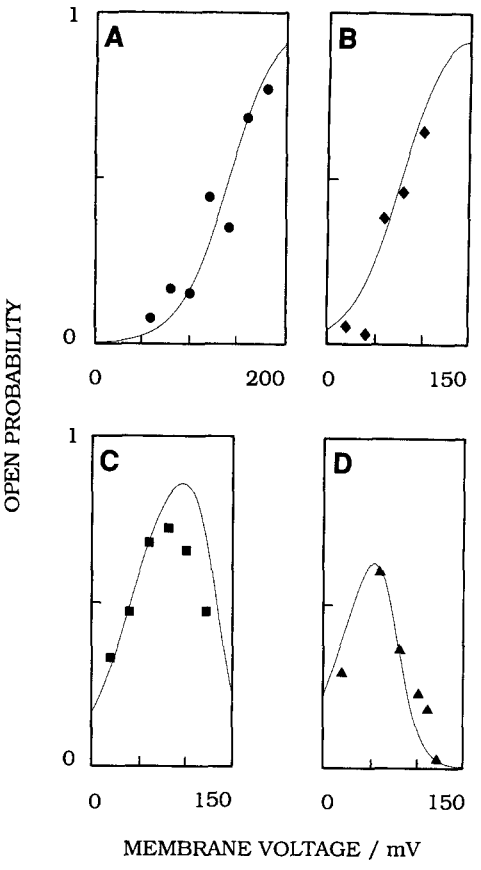

Fig. 6. Voltage and calcium dependence of channel open probability (P_O). Each panel represents summary results for the experiments illustrated in the corresponding panel of Fig. 1. Points were calculated from the data, analyzed for $'P_O$ and K_I via the beta distribution (as in Fig. 3) and Eq. (5a), and analyzed for P_{O+I} via the histograms (as in Fig. 5) and Eq. (8). Smooth curves were drawn by fitting Eq. (7b) to the points, with optimized values of K_G and K_B. This figure quantifies the main features of voltage- and calcium-dependent gating of the yeast K^+ channel, which are qualitatively evident in Fig. 1.

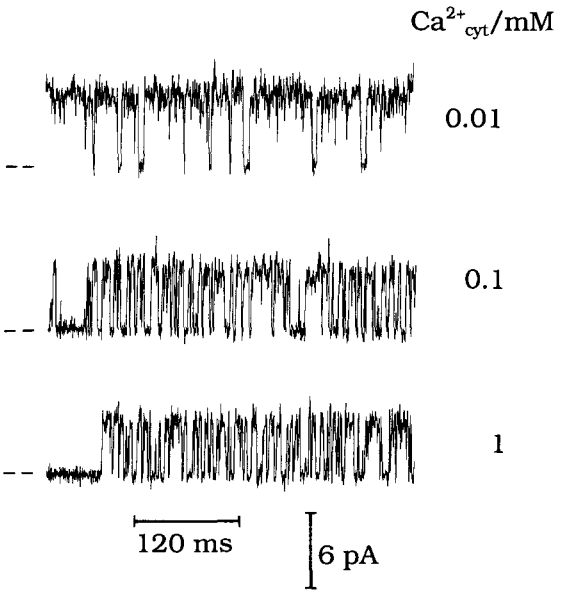

Fig. 7. Demonstration that calcium-induced blocking events (*B*) increase primarily in *frequency*, not in duration, with rising cytoplasmic $[Ca^{2+}]$. Expanded scale records from a single-channel patch; experiment similar to that in Fig. 1*B–D*. Clamped membrane voltage, +80 mV. Calcium concentrations as shown. Note also that open-channel currents are flickery, indicating that fast interrupts (*I*) continue whenever the channel is not blocked by calcium.

rameter values can be estimated by empirical fitting the plots of Fig. 6 with Eq. (7b). Good fits were obtained only when V_m and $[Ca^{2+}]_{cyt}$ were entered with the signs and stoichiometries shown in Fig. 2. The stability constants can then be written

$$K_G = \frac{K_G^0}{[Ca^{2+}] \cdot e^{zu}} \tag{10a}$$

and

$$K_B = K_B^0 \cdot ([Ca^{2+}] \cdot e^{zu})^2. \tag{10b}$$

In other words, K_G is *inversely* proportional to $[Ca^{2+}]_{cyt}$ and to the Boltzmann expression, and K_B is *directly* proportional to the *square* of those functions. [K_G^0 and K_B^0 are defined for the standard condition that $V_m = 0$ and $[Ca^{2+}]_{cyt} = 1$ M.] Using $K_I^0 = 3.3$ (*see* Eq. (4)), substituting Eqs. (10) into Eq. (7b), and fitting the resultant equation to the data of Fig. 6 yielded $K_G^0 = 1.9 \cdot 10^{-4}$ M and $K_B^0 = 2.7 \cdot 10^3$ M^{-2}, and gave the smooth curves of Fig. 6. Fitting the plot of Fig. 6*A* meant also picking the concentration of calcium, since those data represent a cell-attached experiment. With K_G and K_B determined from the fits of Fig. 6*B–D*, the necessary $[Ca^{2+}]_{cyt}$ was 0.7 μM.

Intuitively, it can be seen that the form of K_G and the value of K_G^0 are determined by the rising curve of open probability (P_O) *vs.* V_m at moderate positive voltages; and that the form of K_B and value of K_B^0 are determined by the amplitude cutoff and descending slope of P_O at higher positive voltages.

In order to decompose the stability constants K_G and K_B into their constituent unidirectional rate constants, additional information is needed. More careful inspection of the records in Fig. 1 (and related data) made clear that the extent of V_m-dependent Ca^{2+} blocking was determined largely by the *frequency* of calcium-induced blocks, not by their duration, which was rather independent of both V_m and $[Ca^{2+}]_{cyt}$, as shown by the several expanded records in Fig. 7. The duration of blocking events,

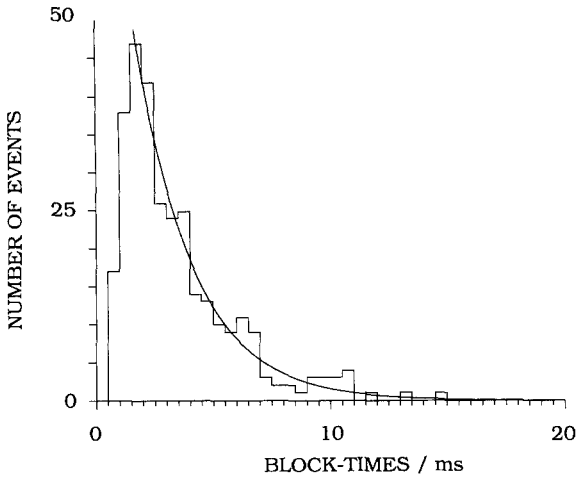

Fig. 8. Dwell-time histogram for calcium-induced block of the channel, indicating simple exponential decay of the blocked state. Single-channel patch from experiment similar to that in Fig. 1*D*, with membrane voltage clamped at +100 mV. The smooth curve represents optimized fitting of the exponential distribution function, with a mean closed time (τ_B) of 2.5 msec. Events shorter than 1 msec were omitted from the fit.

Table 1. Kinetic parameters for the voltage- and calcium-dependent channel blocks

V_m (mV)	Parameter	$[Ca^{2+}]_{cyt}$ (mM):	
		0.1	1.0
80	K_B	0.02	1.7
	τ_B (msec)	2.1	2.6
	k_{BO} (sec^{-1})	476	385
	k_{OB} (sec^{-1})	9.5	655
100	K_B	0.07	8.6
	τ_B (msec)	2.8	2.5
	k_{BO} (sec^{-1})	357	400
	k_{OB} (sec^{-1})	26.5	3,440
120	K_B	0.4	43
	τ_B (msec)	2.8	2.7
	k_{BO} (sec^{-1})	357	370
	k_{OB} (sec^{-1})	143	15,900

K_B = stability constant for the blocked state, determined by fitting Eq. (7b) to the plots in Fig. 6. τ_B = mean closed time for the blocked state, obtained by fitting a simple exponential probability density function to dwell-time histograms, similar to that of Fig. 8. k_{BO} = rate constant for channel opening from the blocked state, $= 1/\tau_B$. k_{OB} = rate constant for channel closing to the blocked state, $= K_B/\tau_B$. For the blocking reaction, all voltage and calcium dependence is in k_{OB}, which is equal to $k^0_{OB}\{[Ca^{2+}]_{cyt} \cdot \exp(eV/kT)\}^2$, where $k^0_{OB} \cong 1.3 \cdot 10^6$ sec^{-1} M^{-2}, averaged for the six cases in this table (*see also* Eq. 10b).

for example at +100 mV and 1 mM Ca^{2+}, is displayed in the histogram of Fig. 8, which represents simple exponential decay of a blocked state having a mean dwell-time (τ_B) of 2.5 msec. As can be seen from Table 1, there was random variation of this value for the different experimental conditions, but τ_B averaged 2.5 msec overall, corresponding to a transition probability $B \rightarrow O$ ($k_{BO} = 1/\tau_B$) of 400 sec^{-1}. Individual values for k_{BO} are also shown in Table 1, along with the voltage- and calcium-dependent values of k_{OB} ($= K_B/k_{BO}$). The implied average value of k^0_{OB}—for standard conditions ($V_m = 0$, $[Ca^{2+}]_{cyt} = 1$ M)—is $1.3 \cdot 10^6$ sec^{-1} M^{-2}.

We cannot analogously obtain values for k_{GO} and k_{OG}, because the mean lifetime of the *G*-state is too long to allow accumulation of sufficient data for convincing dwell-time histograms. Qualitatively, however, τ_G ($= 1/k_{GO}$) is in the range of several hundred msec at moderate positive voltages and 10 μM Ca^{2+}, but is both voltage and calcium dependent (*see* Fig. 1).

Open-Channel Currents

As has already been discussed (*see* Eq. (1) and Fig. 3), the time-averaged effect of unresolved channel interrupts diminished the apparent open-channel current in most records of this yeast plasma membrane K^+ channel. But a fringe benefit of the beta distribution analysis is that it enables the value of I_o, the true open-channel current, to be estimated. Values of I_o for the conditions shown in Fig. 1 are plotted in Fig. 9. Current tended toward *saturation* at large positive voltages, and probably also at large negative voltages (but the paucity of channel-open events at negative voltages obviously makes that a weak statement). Permeation, then, is easily *described* by a simple reaction cycle analogous to conventional enzyme kinetics (*see* Materials and Methods).

Equation (2) was fitted by least squares to all data in Fig. 9 with the actual rate constants, $k^0_{io} = 57.4$, $k^0_{oi} = 33.2$, $\kappa_{io} = 43.1$, and $\kappa_{oi} = 31.6$, in units of $10^6 \cdot sec^{-1}$, for the 10 μM data (●) and a scaling factor of 0.84 for a 10-fold increase in free Ca^{2+}. Evidently, increased cytoplasmic Ca^{2+} causes only a weak and voltage-independent reduction in open-channel currents, but did *not* influence the tendency of I_O to saturate at large membrane voltages. The maximal slope conductance (G_{max}) of these K^+ channels, observed near the reversal voltage (V_m intercept in Fig. 9), was ~63 pS with {200 K^+/50 K^+} for inside-out patches.

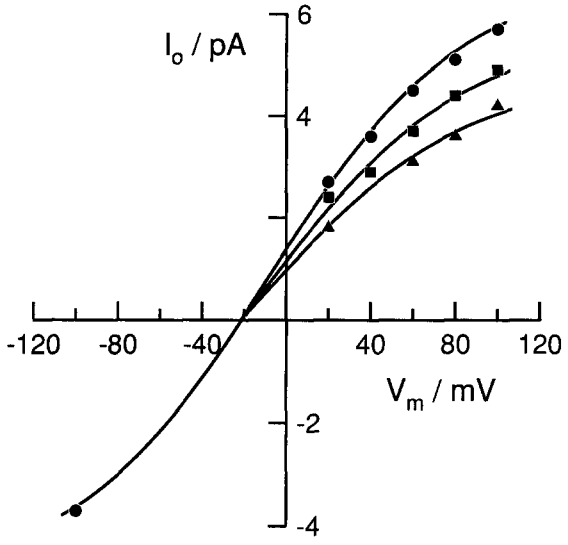

Fig. 9. Open-channel current-voltage plots for yeast K^+ channels, showing the tendency of current to saturate at large positive voltages. Recording conditions as in Fig. 1, with 10 μM Ca^{2+} (●), 100 μM Ca^{2+} (■), and 1 mM Ca^{2+} (▲). Data over the full span (10 μM Ca^{2+}) were fitted by text Eq. (2), and the positive portion of the curve was scaled by factors of 0.84 and 0.70, respectively, to fit the data at 100 μM and 1 mM Ca^{2+}.

Time-Averaged Currents

All K^+ channels observed in these experiments appeared to have the same gating and conductances properties. If that observation can be extrapolated to intact cells, passive K^+ conductance of the *Saccharomyces* plasma membrane due to the total ensemble of these channels can be inferred from time-averaged behavior of single channels observed in isolated patches. That time-averaged behavior is the product of open-channel current and open probability ($I_o \cdot P_o$) as a function of V_m, $[Ca^{2+}]_{cyt}$, etc., and can be computed by dividing the fitted curves in Fig. 9 by the appropriate value of $(1 + K_I + K_G + K_B)$ from Eq. (7b). The resultant currents are *plotted* against membrane voltage for each of the three calcium concentrations tested, in Fig. 10, and smooth curves have been drawn as the product of Eq. (7b) and Eq. (2), using the numerical values of parameters determined as above. Thus, despite the monotonic character of unitary currents through this K^+ channel (Fig. 9), the expected whole-membrane currents decline sharply for elevated (+) membrane voltages and calcium concentrations, due entirely to effects of V_m and $[Ca^{2+}]$ on P_o.

Discussion

The salient features of the *Saccharomyces* plasma membrane K^+ channel, apart from its predominant K^+ selectivity, are that (i) under the conditions used here, it appears closed at negative membrane voltages and is opened by positive polarization of the plasmalemma; (ii) it has two distinct voltage-dependent gating modes, with apparently a single open state but two closed states (*I*, *G*) having mean lifetimes of several hundred *micro*seconds (*I*) and several hundred *milli*seconds (*G*), respectively; (iii) combined *I*- and *G*-gating yields a characteristic "bursting" behavior of channel openings; (iv) moderately elevated cytoplasmic calcium (*ca.* 10 μM) antagonizes the *G*-state, thus increasing channel open probability; and finally (v) high cytoplasmic calcium concentrations (100 μM and above) cause stochastic blocking of the channel, which is exaggerated at strong positive membrane voltages (i.e., > +60 mV); this phenomenon defines a third closed state (*B*) of the channel. A simple reaction model to describe the behavior of this K^+ channel has been drawn in Fig. 2. Alternative serial models have been examined as well, but discarded for, e.g., the following reason. The integer relationships for Ca^{2+} binding (0 for $O \rightarrow I$, 1 for $O \rightarrow G$, and 2 for $O \rightarrow B$) as well as for the apparent charge numbers for the voltage sensitivities (1 for $O \leftrightarrow I$, 1 for $O \leftrightarrow G$, and 2 for $O \leftrightarrow G$) are consistent with the parallel model, but incompatible with serial models, where coupling between the individual reactions leads to intermediate relationships. The reaction parameters of the parallel model (Fig. 2) which can be determined from the accumulated data are summarized in Table 2, and the extended voltage dependence of the channel, based on these parameters, is displayed in Fig. 11.

Open-channel currents through the yeast K^+ channel were sigmoidal as a function of membrane voltage (Fig. 9). These characteristics are confirmed by the data in Fig. 1*A*, where open-channel currents do not significantly increase any more upon an increase in voltage from 180 to 200 mV. Saturation of open-channel currents is a common observation in isolated-patch studies of plant K^+ channels, when a wide voltage span is tested (Schroeder, Hedrich & Fernandez, 1984; Lühring, 1986; Bertl, 1989; Katsuhara, Mimura & Tazawa, 1989; Fairley, Laver & Walker, 1991; Spalding et al., 1992). A generic restatement of this finding is that transiting ions have a finite residence time in/on the channel, independent of the electric field. Although a more detailed study would be required to demonstrate that saturation arises in the channel itself, rather than in an access region (Adrian, 1969; Läuger, 1976), the behavior is clearly reminiscent of that almost univer-

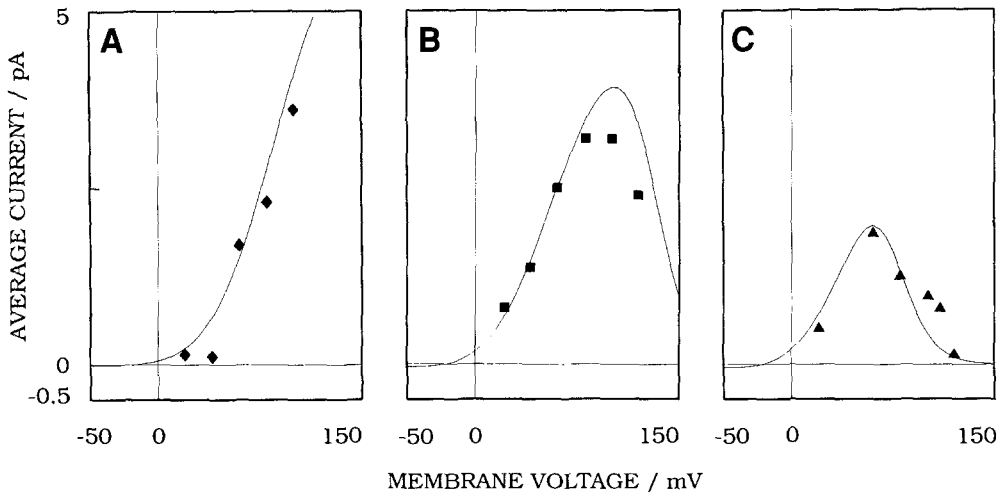

Fig. 10. Time-averaged currents through the yeast K^+ channel, demonstrating a prominent decline of current at high (+) voltages and high cytoplasmic [Ca^{2+}], due mainly to calcium-induced block. Panels *A*, *B*, and *C*, respectively, correspond to Fig. 6*B*, *C*, and *D*, with 10 μM, 100 μM, and 1 mM Ca^{2+}. Plotted points were obtained as the product of plotted values of P_O in Fig. 6 times the plotted values of I_o in Fig. 9. The smooth curves were drawn as the product of P_O (Eq. 7b) and I_o (Eq. 2) with the fitted parameters given in the text for Fig. 9, and I_o scaling factors 1, 0.84, and 0.70, respectively, for panels *A*, *B*, and *C*.

sally observed in carrier-mediated processes. And these are customarily described *and* analyzed in terms of enzyme-like cyclic reactions. For monotonic current-voltage data, indeed, only a two-state cyclic reaction scheme—with a single voltage-dependent step—is required (Hansen et al., 1981), and the use of such a function (Eq. 2) can be taken conservatively as providing an empirical description, plus a simple method to interpolate or extrapolate from the data.

It is our opinion that this representation is conceptually simpler than diffusional barrier models for channel transport which do display saturating currents (Heckmann et al., 1972; French & Shoukimas, 1985). Furthermore, since gated channels are universally accepted to undergo "conformational" changes in the gating process (Catterall, 1977; Läuger, 1983; McCleskey & Almers, 1985; Ring & Sandblom, 1988; Eisenberg, 1990), it is no great leap to suppose that they also change conformations (or at least electrostatic configurations) during actual ion transit. This concept, indeed, underlies Läuger's (1980) unifying idea of active transport as energy-driven channel peristalsis. While it must be allowed that most channels display apparent multiple simultaneous occupancy by transiting ions, that in itself does not rule out configurational changes in the channel molecule nor invalidate the use of enzyme-type kinetics to describe the process (Läuger, 1983). Indeed, at least one well-known "file-diffusion" phenomenon, the anomalous mole-fraction effect observed in channel transport of ion mixtures, can be *better* described by a cyclic enzyme-type reaction with current carried across a *single* energy barrier (K^+/Tl^+ currents through *Nitella* K^+ channels; Draber et al., 1991, *see also* Markin et al., 1992) than by the multiple-ion, multiple-barrier pore model of Hille and Schwarz (1978).

Open-Channel Current Versus Time-Averaged Current

In the enzyme-kinetic approach to channel-type transport, the sigmoidal current-voltage characteristic of an open channel corresponds to the fundamental reaction cycle of an ordinary enzyme, and current saturation at V_m displacements far from the zero-current voltage is equivalent to velocity saturation (V_{max}) in the conventional Michaelis-Menten analysis. But modulation of enzyme activity, which in the case of individual ion channels would be due to changes in on/off kinetics of the fundamental reaction cycle, produces additional phenomena. For example, after appearing to saturate with rising V_m, current can decline again at still higher voltages ($G = dI_o/dV_m < 0$), thus showing negative slope conductance; or the slope can rise continuously with increasing voltage ($dG/dV_m > 0$), an effect which has been termed "superlinearity." All three types of current-voltage characteristics are visible in data for the yeast plasma-membrane K^+ channel: *saturation*, in the open-channel current-voltage characteristics of Fig. 9; *negative slope conductance*, in the time-averaged current-voltage curves at high calcium concentrations (Fig. 10*B*,*C*), due to block of

Table 2. Summary of determined reaction parameters for *Saccharomyces* plasma-membrane K^+ channel

Part A: Gating Parameters[a]

Closed state	Parameter	Standard value[b]	Voltage dependence	Calcium dependence
Interrupt	τ_O (msec)	0.17	$e^{0.71zu}$	
	τ_I (msec)	0.58	$e^{-0.29zu}$	
	K_I	3.3	$(e^{zu})^{-1}$	
Gap	τ_G (msec)	$1.4 \cdot 10^2$	Yes, but forms undetermined	
	K_G (M)	$1.9 \cdot 10^{-4}$	$(e^{zu})^{-1}$	$[Ca^{2+}]^{-1}$
Block	τ_B (msec)	2.5		
	K_B (M^{-2})	$2.7 \cdot 10^3$	$(e^{zu})^2$	$[Ca^{2+}]^2$
	k_{OB} ($sec^{-1} \cdot M^{-2}$)	$1.3 \cdot 10^6$	$(e^{zu})^2$	$[Ca^{2+}]^2$

Part B: Transport Parameters[c]

Direction	Parameter	Standard value	Voltage dependence
Outward	k_{io}	$57.4 \cdot 10^6$ (sec^{-1})	$e^{0.5zu}$
	κ_{io}	$43.1 \cdot 10^6$ (sec^{-1})	
Inward	k_{oi}	$33.2 \cdot 10^6$ (sec^{-1})	$e^{-0.5zu}$
	κ_{oi}	$31.6 \cdot 10^6$ (sec^{-1})	

[a] Model of Fig. 2, assumes three closed states in parallel, and a single open state.
[b] For voltage-, calcium-dependent parameters, standard values are defined as those for which $V_m = 0$, $[Ca^{2+}]_{cyt} = 1$ M.
[c] Calculated from Eq. (2), for a two-state cyclic reaction model, fitted to the sigmoid plots of Fig. 9. Charge transported by the transiting cations. u, the "reduced" membrane voltage, is defined by $u = eV_m/kT$. The τ's—mean lifetimes—were determined as described for Fig. 3, Fig. 8, and Table 1, and are reciprocals of rate constants set out in Fig. 2: $\tau_O = 1/k_{OI}$; $\tau_I = 1/k_{IO}$; $\tau_G = 1/k_{GO}$; $\tau_B = 1/k_{BO}$.

the cycle by Ca^{2+}; and *superlinearity*, at low calcium concentrations and voltages (Fig. 10*A*), resulting from an increase of the open times (for positive-going V_m) and a decrease of closed times within the bursts. Thus, both negative slope conductances and steadily rising slope conductances, which have been treated previously for steady-state conditions (*see, e.g.*, Bertl, 1989; Laver, 1990; Laver & Walker, 1991), are demonstrated here and are explained in terms of specific modulation of the gating of single channels, resulting from antagonistic interactions of V_m and ligands (here $[Ca^{2+}]_{cyt}$) over different voltage and concentration ranges.

Calcium Dependence of Gating

The biphasic effect of calcium on the yeast K^+ channel, as summarized in the P_o plots of Fig. 11, is unusual among reports on non-animal cells, but that probably reflects the fact that the Ca^{2+} dependencies described for other plant channels have generally been observed over a narrow, quasiphysiological range of concentrations. Ca^{2+} *inhibition* of an inward rectifying K^+ channel in *Vicia* guard cells (Schroeder & Hagiwara, 1989), for example, and Ca^{2+} *activation* of anion channels in *Amaranthus* and *Vicia* (Boult et al., 1989; Schroeder & Hagiwara, 1989; Hedrich, Busch & Raschke, 1990), have all been reported to be monotonic, but for concentrations between 0.01 and 1.5 μM in controlled experiments on *Vicia*, and up to 10 μM on *Amaranthus*. Both aspects of the inhibitory component of elevated $[Ca^{2+}]$ visible in Fig. 11: the decreasing P_o with increasing (+) V_m, and the decreasing amplitude of peak P_o, are directly attributable to the blocking events (*B*-closures), and it seems likely that such events will also be found in plant channels if high calcium concentrations are used.

Dual effects of calcium—activation and blockade—are well known and widely distributed among channels in animal-cell membranes (Latorre et al., 1989). Calcium-activated maxi-K^+ channels often display $[Ca^{2+}]$-dependent closures of >100 msec duration, which resemble the well-known barium blockade of the channels (Vergara & Latorre, 1983; Findlay, Dunne & Petersen, 1985). In some cases such blockade is enhanced by positive membrane voltage

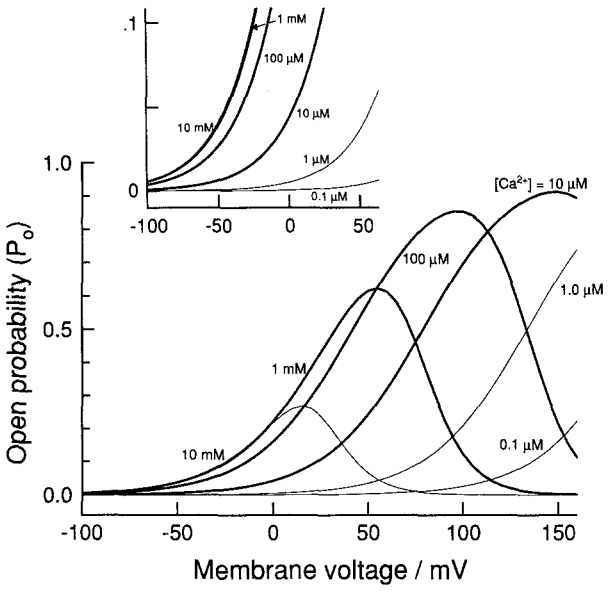

Fig. 11. Summary description of open probability of the *Saccharomyces* K^+ channel: voltage and calcium dependence. Curves computed from text Eq. (7b), with the values for closed-state stability constants (K_I, K_G, K_B) given in Table 2. Bold lines represent results for calcium concentrations actually tested (10 μM–1 mM), and fine lines represent predictions for useful calcium concentrations yet to be tested (0.1 μM, 1μM, and 10 mM). Inset: five-fold expansion of P_O scale, to resolve behavior at negative membrane voltages.

and by lowered $[K^+]$, suggesting the block to result from calcium occupancy of K^+-binding sites rather than from modulation of a separate gate. From a quantitative kinetic viewpoint, however, Ca^{2+}-dependent block of maxi-K^+ channels is rather different from that seen in yeast K^+ channels, which shows increasing frequency of *brief* (2–3 msec) closures with elevated calcium. The yeast channels also show the same blocking behavior with elevated cytoplasmic magnesium (A. Bertl, *unpublished experiments*), but at 30-fold higher concentrations than are needed for calcium.

Kinetic evidence thus far would permit the two actions of Ca^{2+} ions on the yeast channel, activation and blockade, to be mechanistically distinct; i.e., with the $G \rightarrow O$ transition reflecting chemical gating, and the $O \rightarrow B$ transition reflecting Ca^{2+} occlusion of K^+-binding/transport site(s) within the channel. In most cases, Ca^{2+} blockade is fast, allowing just an apparent reduction in unitary currents to be observed. However, this blockade seems to be slow in *Saccharomyces,* resulting in discrete events, which can be resolved on a time scale of msec. Independence of activation and blockade was long assumed for the related effects of Ca^{2+} on both Na^+ and K^+ channels in squid axon (*see review* in Armstrong & Matteson, 1986), even though evident competitive interaction of the transported ions with calcium in the *gating* process suggested a unified mechanism. Direct support for a unified Ca^{2+} effect on Na^+ channels (in GH3 cells, a cultured pituitary line) was recently obtained by demonstration of a linear proportionality between the Ca^{2+}-induced shift of gating voltage and Ca^{2+}-induced reduction in amplitude of whole-cell Na^+ currents (Armstrong & Cota, 1991). Ca^{2+}-blocking events, as those in the yeast K^+ channel, display several properties expected for reaction with binding sites within the channel, including voltage dependence and multiple-site action (French & Shoukimas, 1985; Moczydlowski, 1986). If this notion withstands further tests, e.g. inhibition by permeant extracellular (*trans*) ions, or selective reaction with open channels, then the gate-shifting effect might also be generated by an "in-passage" reaction with Ca^{2+}.

Relative Voltage-Dependence of P_O

With $[Ca^{2+}]_{cyt}$ in the physiological range (0.1–0.3 μM; Miller, Vogg & Sanders, 1990; Halachmi & Eilam, 1989; Iida, Yagawa & Anraku, 1990), voltage-dependent opening of the yeast K^+ channel appears pushed surprisingly far into positive voltages (summarized in Fig. 11).

At least two important considerations about the *circumstances* of patch recording bear on the physiological relevance of this observation.

(i) *Density (number per cell) and size* of K^+ channels, relative to other membrane parameters. Typical tight-seal patches from *Saccharomyces* plasma membrane display 1–3 K^+ channels and have a probable recording area near 5 μm^2. Roughly calculated, then, there should be 1 channel per 2 μm^2 of cell surface, or about 40 channels in an intact yeast cell of normal size (5–6 μm diameter). Fungal plasma-membrane resistivities can exceed 100 k$\Omega \cdot cm^2$ (Blatt & Slayman, 1983), or $\sim 10^{11}$ Ω for normal yeast. Since opening of a single 40 pS K^+ channel would give a cell-membrane resistance of only $2.5 \cdot 10^{10}$ Ω, P_o for these channels under resting conditions should be ~0.006 or smaller. (This only restates in quantitative terms a general principle of channel function: that to be physiologically useful, channels—*by their nature*—must be predominantly closed.)

(ii) *Voltage displacement from* E_{K^+}. It is convenient in patch-clamp experiments to use elevated salt concentrations in both bath and pipette in order to minimize recording series resistance and maximize single-channel currents. In the present experiments we routinely used 200 mM bath (cytoplasmic) KCl and 50 mM pipette (outside) KCl, so that $E_{K^+} \approx$

−29 mV. Under ordinary growth conditions $[K^+]_{out}$ can easily go below 1 mM, which would shift E_{K^+} to the neighborhood of −120 mV. This raises the question, applicable to free-living organisms in general, of whether the important voltage-gating parameter is absolute V_m, as plotted in Figs. 1, 4, 6, 10, and 11, or $[V_m - E_{K^+}]$, the so-called disequilibrium voltage for potassium. While most of the single-channel literature focuses on absolute voltage, it has often been noted that whole-cell ionic conductances, particularly for potassium, behave as if $[V_m - E_{K^+}]$, were the important gating parameter. Thus, Ciani et al. (1978) coined the descriptive "electrochemical-potential-dependent gating" in modeling anomalous rectification (K^+) in *Nordora* eggs (starfish; Hagiwara & Takahashi, 1974), taking off from earlier observations on striated muscle (Hodgkin & Horowicz, 1959; Nakamura, Nakajima & Grundfest, 1965; Adrian, 1969). Related effects of the electrochemical gradient for Cl^-, upon gating modes of Cl^- channels, have recently been described in *Torpedo* electroplax (Richard & Miller, 1990).

For the yeast plasma-membrane K^+ channel, preliminary experiments with varying cytoplasmic and external K^+ suggest that $[V_m - E_{K^+}]$ is indeed the relevant gating parameter. With a 10-fold K^+ gradient (500 mM/50 mM or 200 mM/20 mM) considerable channel activity exhibiting positive open-channel currents can be seen at voltages as negative as −40 mV (A. Bertl, *unpublished experiments*). Therefore, lowering $[K^+]_{out}$ to the physiologically relevant range (1–10 mM) would move the curves of Fig. 11 significantly to the left.

Functions of the Yeast K^+ Channel

Although the yeast K^+ channel does not show rectification in the open-channel current-voltage characteristics, it must nevertheless be classified as an outward rectifying K^+ channel, because of its time-averaged characteristic (Fig. 10, rising limbs of all three curves). The time-averaged single-channel current is comparable to whole-cell currents, and is therefore the physiologically important characteristic.

Outward-rectifying K^+ channels—variously known as I_{K^+} channels, $I_{K^+_{out}}$ channels, and seen in such guises as delayed rectifiers, or slow-K^+ channels—are a common feature of both animal and plant plasma membranes (Latorre & Miller, 1983; Hille, 1984; Hedrich & Schroeder, 1989; Tester, 1990). In the excitable membranes of nerve and muscle, activation of outward-rectifying K^+ channels speeds repolarization of the membrane during action potentials. $I_{K^+_{out}}$ channels in plant cells probably also play that same role, but activate in response to depolarization on a time scale appropriate for plant action potentials, i.e., 1–10 sec (Kitasato, 1973; Bertl & Gradmann, 1987; Iijima & Hagiwara, 1987; Bertl et al., 1988; Schroeder, 1989), rather than the 1–10 msec of most nerve and muscle membranes. In fungi, too, $I_{K^+_{out}}$ channels could function to repolarize the membrane following action potentials (Fuller & Pickard, 1972; Slayman et al., 1976, Müller, Malchow & Hartung, 1986), with consequences either for signaling or—because of the long duration of the action potentials—for turgor regulation (Slayman, 1992). Reliable direct voltage measurements in *Saccharomyces* are technically difficult, however, and action potentials have not yet been reported from this organism. At present, therefore, we can only speculate on the involvement of outward-rectifying K^+ channels in action potentials and turgor regulation in yeast, although the channel described here activates in response to depolarization on a time-scale comparable to that of plant $I_{K^+_{out}}$ channels.

However, the combination of voltage modulation of yeast plasma membrane K^+ channels and chemical modulation (i.e., by cytoplasmic Ca^{2+}) provides a wide range of possible physiological responses by the channels, and is likely to account for peculiar flux and voltage effects observed in *Saccharomyces* during mediated uptake of sugars, specifically of monosaccharides *vs.* disaccharides.

Glucose, for example, is taken up by facilitated diffusion without ion coupling (Cirillo, 1961; Heredia et al., 1968; Bisson & Fraenkel, 1982; Cirillo, 1989), and thus without a primary change in membrane voltage. At low extracellular concentrations (≤5 μM), however, glucose uptake is accompanied by K^+ efflux and apparent membrane *hyperpolarization* (Van de Mortel et al., 1988). Glucose influx also stimulates a biphasic rise in cytoplasmic $[Ca^{2+}]$ (Eilam, Othman & Halachmi, 1990), with a fast, transient component probably occurring via influx from the extracellular solution (Eilam & Chernichovsky, 1987; Eilam & Othman, 1990), and a much slower component (lasting 60 min or more) probably occurring by release from internal stores (Eilam & Othman, 1990). Bertl et al. (1992*a*) have pointed out that calcium-, pH-, and redox-regulation of the *Saccharomyces* tonoplast cation channel, which is Ca^{2+} permeable, all make it a likely effector for glucose-induced release of vacuolar Ca^{2+}: sudden feeding of glucose evokes both cytoplasmic alkalinization (Gillies, 1982) and a surge of reducing equivalents (NADH; Ghosh & Chance, 1964; Polakis & Bartley, 1966). Furthermore, in cells with resting plasma membrane voltages positive to E_{K^+} (e.g., with micromolar external K^+) rising cytoplasmic Ca^{2+} could activate plasma membrane K^+

channels and thus explain both the glucose-associated K^+ efflux and the apparent hyperpolarization. On the other hand, uptake of maltose, a disaccharide, has also been reported to activate passive K^+ efflux from *Saccharomyces* (Serrano, 1977), but maltose uptake occurs via an H^+-coupled symport system which itself is depolarizing (Serrano, 1977). In this case, sufficient depolarization per se would activate the plasma membrane K^+ channel.

The authors are indebted to Dr. Michael Snyder and Dr. Constance Copeland (Yale Department of Biology) for providing the tetraploid yeast strain and for initial assistance in handling the cells and preparing protoplasts; and to Dr. Esther Bashi for technical assistance throughout the experiments. The work was supported by Research Grant 85ER13359 from the United States Department of Energy (to C.L.S.), by Forschungs-Stipendium Be 1181/2-1 from the Deutsche Forschungsgemeinschaft (to A.B.), and by Akademie-Stipendium II/66647 from the Volkswagenstiftung (to D.G.).

References

Adrian, R.H. 1969. Rectification in muscle. *Prog. Biophys. Mol. Biol.* **19:**341–369

Anderson, J.A., Huprikar, S.S., Kochian, L.V., Lucas, W.J., Gaber, R.F. 1992. Functional expression of a probable *Arabidopsis thaliana* potassium channel in *Saccharomyces cerevisiae*. *Proc. Natl. Acad. Sci. USA* **89:**3736–3740

Armstrong, C.M., Cota, G. 1991. Calcium ion as a cofactor in Na channel gating. *Proc. Natl. Acad. Sci. USA* **88:**6528–6531

Armstrong, C.M., Matteson, D.R. 1986. The role of calcium ions in the closing of K channels. *J. Gen. Physiol.* **87:**817–832

Bertl, A. 1989. Current-voltage relationships of a sodium-sensitive potassium channel in the tonoplast of *Chara corallina*. *J. Membrane Biol.* **109:**9–19

Bertl, A., Gradmann, D. 1987. Current-voltage relationships of potassium channels in the plasmalemma of *Acetabularia*. *J. Membrane Biol.* **99:**41–49

Bertl, A., Gradmann, G., Slayman, C.L. 1992*a*. Calcium- and voltage-dependent ion channels in *Saccharomyces cerevisiae*. *Philos. Trans. R. Soc. London B.* **338:**63–72

Bertl, A., Blumwald, E., Coronado, R., Eisenberg, R., Findlay, G., Gradmann, D., Hille, B., Köhler, K., Kolb, H.-A., MacRobbie, E., Meissner, G., Miller, C., Neher, E., Palade, P., Pantoja, O., Sanders, D., Schroeder, J., Slayman, C.L., Spanswick, R., Williams, A. 1992*b*. Electrical measurements on endomembranes. *Science* **258:**873–874

Bertl, A., Klieber, H.G., Gradmann, D. 1988. Slow kinetics of a potassium channel in *Acetabularia*. *J. Membrane Biol.* **102:**141–152

Bertl, A., Slayman, C.L. 1990. Cation-selective channels in the vacuolar membrane of *Saccharomyces:* Dependence on calcium, redox state, and voltage. *Proc. Natl. Acad. Sci. USA* **87:**7824–7828

Bertl, A., Slayman, C.L. 1993. Complex modulation of cation channels in the tonoplast and plasma membrane of *Saccharomyces cerevisiae:* Single-channel studies. *J. Exp. Biol.* **172:**271–287

Bisson, L.F., Fraenkel, D.G. 1982. Involvement of kinases in glucose and fructose uptake by *Saccharomyces cerevisiae*. *Proc. Natl. Acad. Sci. USA* **80:**1730–1734

Blatt, M.R., Slayman, C.L. 1983. KCl leakage from microelectrodes and its impact on the membrane parameters of a nonexcitable cell. *J. Membrane Biol.* **72:**223–234

Boult, M., Elliott, D.C., Findlay, G.P., Terry, B.R., Tyerman, S.D. 1989. A multi-state anion channel in the plasmalemma of *Amaranthus tricolor*. *In:* Plant Membrane Transport: The Current Position. J. Dainty, M.I. de Michelis, E. Marrè, and F. Rasi-Caldogno, editors; pp. 517–520. Elsevier, Amsterdam

Caldwell, J.H., VanBrunt, J., Harold, F.M. 1986. Calcium-dependent anion channel in the water mold, *Blastocladiella emersonii*. *J. Membrane Biol.* **89:**85–97

Camancho, M., Ramos, J., Rodriguez-Navarro, A. 1981. Potassium requirements of *Saccharomyces cerevisiae*. *Curr. Microbiol.* **6:**295–299

Catterall, W.A., 1977. Activation of the action potential Na^+ ionophore by neurotoxins: An allosteric model. *J. Biol. Chem.* **23:**8669–8676

Ciani, S., Krasne, S., Miyazaki, S., Hagiwara, S. 1978. A model for anomalous rectification: Electrochemical-potential-dependent gating of membrane channels. *J. Membrane Biol.* **44:**103–134

Cirillo, V.P. 1961. Sugar transport in microorganisms. *Annu. Rev. Microbiol.* **15:**197–218

Cirillo, V.P. 1989. Sugar transport in normal and mutant yeast cells. *Meth. Enzymol.* **174:**617–622

Draber, S., Schultz, R., Hansen, U.-P. 1991. Patch-clamp studies on the anomalous mole fraction effect of the K^+ channel in cytoplasmic droplets of *Nitella:* An attempt to distinguish between a multi-ion single-file pore and an enzyme kinetic model with lazy state. *J. Membrane Biol.* **123:**183–190

Eilam, Y., Chernichovsky, D. 1987. Uptake of Ca^{2+} driven by the membrane potential in energy-depleted yeast cells. *J. Gen. Microbiol.* **133:**1641–1649

Eilam, Y., Othman, M. 1990. Activation of Ca^{2+} influx by metabolic substrates in *Saccharomyces cerevisiae:* role of membrane potential and cellular ATP levels. *J. Gen. Microbiol.* **136:**861–866

Eilam, Y., Othman, M., Halachmi, D. 1990. Transient increase in Ca^{2+} influx in *Saccharomyces cerevisiae* in response to glucose: effects of intracellular acidification and cAMP levels. *J. Gen. Microbiol.* **136:**2537–2543

Eisenberg, R.S. 1990. Channels as enzymes. *J. Membrane Biol.* **115:**1–12

Fairley, K., Laver, D., Walker, N.A. 1991. Whole-cell and single-channel currents across the plasmalemma of corn shoot suspension cells. *J. Membrane Biol.* **121:**11–22

Findlay, I., Dunne, M.J., Petersen, O.H. 1985. High-conductance K^+ channel in pancreatic islet cells can be activated and inactivated by internal calcium. *J. Membrane Biol.* **83:**169–175

French, R.J., Shoukimas, J.J. 1985. An ion's view of the potassium channel. The structure of the permeation pathway as sensed by a variety of blocking ions. *J. Gen. Physiol.* **85:**669–698

Fuller, F.B., Pickard, B.G. 1972. Spontaneous electrical activity in *Coprinus*. *Z. Pflanzenphysiol.* **67:**291–292

Gaber, R.F., Styles, C.A., Fink, G.R. 1988. *TRK1* encodes a plasma membrane protein required for high-affinity potassium transport in *Saccharomyces cerevisiae*. *Mol. Cell. Biol.* **8:**2848–2859

Ghosh, A., Chance, B. 1964. Oscillations of glycolytic intermediates in yeast cells. *Biochem. Biophys. Res. Comm.* **16:**174–181

Gillies, R.J. 1982. Intracellular pH and proliferation in yeast, *Tetrahymena* and sea urchin eggs. *In:* Intracellular pH: Its Measurement, Regulation, and Utilization in Cellular Func-

tions. R. Nuticelli and D.W. Deamer, editors; pp. 341–359. A.R. Liss, New York

Gómez-Lagunas, F., Peña, A., Liévano, A., Darszon, A. 1989. Incorporation of ionic channels from yeast plasma membranes into black lipid membranes. *Biophys. J.* **56:**115–119

Gradmann, D., Klieber, H.-G., Hansen, U.-P. 1987. Reaction kinetic parameters for ion transport from steady-state current-voltage curves. *Biophys. J.* **51:**569–585

Gustin, M.C., Martinac, B., Saimi, Y., Culbertson, M.R., Kung, C. 1986. Ion channels in yeast. *Science* **233:**1195–1197

Gustin, M.C., Zhou, X.-L., Martinac, B., Kung, C. 1988. A mechanosensitive ion channel in the yeast plasma membrane. *Science* **242:**762–765

Hagiwara, S., Takahashi, K. 1974. The anomalous rectification and cation selectivity of the membrane of a starfish egg cell. *J. Membrane Biol.* **81:**61–80

Halachmi, D., Eilam, Y. 1989. Cytosolic and vacuolar Ca^{2+} concentrations in yeast cells measured with the Ca^{2+}-sensitive fluorescence dye indo-1. *FEBS Lett.* **256:**55–61

Hamill, O.P., Marty, A., Neher, E., Sakmann, B., Sigworth, F.J. 1981. Improved patch-clamp techniques for high-resolution current recording from cells and cell-free membrane patches. *Pfluegers Arch.* **391:**85–100

Hansen, U.-P., Gradmann, D., Sanders, D., Slayman, C.L. 1981. Interpretation of current-voltage relationships for "active" ion transport systems: I. Steady-state reaction-kinetic analysis of Class-I mechanisms. *J. Membrane Biol.* **63:**165–190

Heckmann, K, Lindemann, B., Schnakenberg, J. 1972. Current-voltage curves of porous membranes in the presence of pore-blocking ions. *Biophys. J.* **12:**683–702

Hedrich, R., Busch, H., Raschke, K. 1990. Ca^{2+} and nucleotide dependent regulation of voltage dependent anion channels in the plasma membrane of guard cells. *EMBO J.* **9:**3889–3892

Hedrich, R., Schroeder, J.I. 1989. The physiology of ion channels and electrogenic pumps in higher plants. *Annu. Rev. Plant Physiol.* **40:**539–569

Heredia, C.F., Sols, A., De la Fuente, G. 1968. Specificity of the constitutive hexose transport in yeast. *Eur. J. Biochem.* **5:**321–329

Hille, B. 1984. Ionic Channels of Excitable Membranes. Sinauer, Sunderland, MA

Hille, B., Schwarz, W. 1978. Potassium channels in multi-ion single-file pores. *J. Gen. Physiol.* **72:**409–442

Hodgkin, A.L., Horowicz, P. 1959. The influence of potassium and chloride ions on the membrane potentials of single muscle fibers. *J. Physiol.* **148:**127–160

Iida, H., Yagawa, Y., Anraku, Y. 1990. Essential role for induced Ca^{2+} influx followed by $[Ca^{2+}]_i$ rise in maintaining viability of yeast cells late in the mating pheromone response pathway: A study of $[Ca^{2+}]_i$ in single *Saccharomyces cerevisiae* cells wth imaging of fura-2. *J. Biol. Chem.* **265:**13391–13399

Iijima, T., Hagiwara, S. 1987. Voltage-dependent K channels in protoplasts of trap-lobe cells of *Dionaea muscipula*. *J. Membrane Biol.* **100:**73–81

Jones, W.B.G., Rothstein, A., Sherman, F., Stannard, J.N. 1965. Variation of K^+ and Na^+ content during the growth cycle of yeast. *Biochim. Biophys. Acta* **104:**310–312

Katsuhara, M., Mimura, T., Tazawa, M. 1989. Patch-clamp study on a Ca^{2+}-regulated K^+ channel in the tonoplast of the brackish characeae *Lamprothamnium succinctum*. *Plant Cell Physiol.* **30:**549–555

Kitasato, H. 1973. K permeability of *Nitella clavata* in the depolarized state. *J. Gen. Physiol.* **62:**535–549

Klieber, H.-G., Gradmann, D. 1993. Enzyme kinetics of the prime K^+ channel in the tonoplast of *Chara:* Selectivity and inhibition. *J. Membrane Biol.* **132:**253–265

Ko, C.H., Buckley, A.M., Gaber, R.F. 1990. *TRK2* is required for low affinity K^+ transport in *Saccharomyces cerevisiae*. *Genetics* **125:**305–312

Ko, C.H., Gaber, R.F. 1991. *TRK1* and *TRK2* encode structurally related K^+ transporters in *Saccharomyces cerevisiae*. *Mol. Cell. Biol.* **11:**4266–4273

Larsson, P., Vacata, V., Lecar, H., Höfer, M. 1992. Multilevel cationic channel in the plasma membrane of *Schizosaccharomyces pombe*. *Biophys. J.* **61:**A512 (*Abstr.* 2957)

Latorre, R., Miller, C. 1983. Conduction and selectivity in potassium channels. *J. Membrane Biol.* **71:**11–30

Latorre, R., Oberhauser, A., Labarca, P., Alvarez, O. 1989. Varieties of calcium-activated potassium channels. *Annu. Rev. Physiol.* **51:**385–399

Läuger, P. 1976. Diffusion-limited ion flow through pores. *Biochim. Biophys. Acta* **455:**493–509

Läuger, P. 1980. Kinetic properties of ion carriers and channels. *J. Membrane Biol.* **57:**163–178

Läuger, P. 1983. Conformational transitions of ionic channels. *In:* Single-Channel Recording. B. Sakmann and E. Neher, editors; pp. 177–189. Plenum, New York

Laver, D.R. 1990. Coupling of K^+-gating and permeation with Ca^{2+} block in the Ca^{2+}-activated K^+ channel in *Chara australis*. *J. Membrane Biol.* **118:**55–67

Laver, D.R., Walker, N.A. 1991. Activation by Ca^{2+} and block by divalent ions of the K^+ channel in the membrane of cytoplasmic drops from *Chara australis*. *J. Membrane Biol.* **120:**131–139

Lühring, H. 1986. Recording of single K^+ channels in the membrane of cytoplasmic drop of *Chara australis*. *Protoplasma* **133:**19–28

Markin, V.S., Liu, D., Gimsa, J., Strobel, R., Rosenberg, M.D., Tsong, T.Y. 1992. Ion channel enzyme in an oscillating electric field. *J. Membrane Biol.* **126:**137–145

McCleskey, E.W., Almers, W. 1985. The calcium channel in skeletal muscle is a large pore. *Proc. Natl. Acad. Sci. USA* **82:**7149–7153

Miller, A.J., Vogg, G., Sanders, D. 1990. Cytosolic calcium homeostasis in fungi: Roles of plasma membrane transport and intracellular sequestration of calcium. *Proc. Natl. Acad. Sci. USA* **87:**9348–9352

Moczydlowski, E. 1986. Single-channel enzymology. *In:* Ion Channel Reconstitution. C. Miller, editor; pp. 75–111. Plenum, New York

Müller, U., Malchow, D., Hartung, K. 1986. Single ion channels in the slime mold *Dictyostelium discoideum*. *Biochim. Biophys. Acta* **857:**287–290

Nakamura, Y., Nakajima, S., Grundfest, H. 1965. Analysis of spike electrogenesis and depolarizing K inactivation in electroplaques of *Electrophorus electricus*, L. *J. Gen. Physiol.* **49:**321–349

Polakis, E.S., Bartley, W. 1966. Changes in the intracellular concentrations of adenosine phosphates and nicotinamide nucleotides during aerobic growth cycle of yeast on different carbon sources. *Biochem. J.* **99:**521–533

Richard, E.A., Miller, C. 1990. Steady-state coupling of ion-channel conformations to a transmembrane ion gradient. *Science* **247:**1208–1210

Ring, A., Sandblom, J. 1988. Modulation of gramicidin A open channel lifetime by ion occupancy. *Biophys. J.* **53:**549–559

Schroeder, J.I. 1989. Quantitative analysis of outward rectifying

K^+ channel currents in guard cell protoplasts from *Vicia faba*. *J. Membrane Biol.* **107:**229–235

Schroeder, J.I., Hagiwara, S. 1989. Cytosolic calcium regulates ion channels in the plasma membrane of *Vicia faba* guard cells. *Nature* **338:**427–430

Schroeder, J.I., Hedrich, R., Fernandez, J.M. 1984. Potassium-selective single channels in guard cell protoplasts of *Vicia faba*. *Nature* **312:**361–362

Sentenac, H., Bonneaud, N., Minet, M., Lacroute, F., Salmon, J.-M., Gaymard, F., Grignon, C. 1992. Cloning and expression in yeast of a plant potassium ion transport system. *Science* **256:**663–665

Serrano, R. 1977. Energy requirements for maltose transport in yeast. *Eur. J. Biochem.* **80:**97–102

Slayman, C.L. 1992. Channels, pumps, and osmotic machines in plants: A tribute to W.J.V. Osterhout. *In:* The Biological Century. R. Barlow, G. Weissmann, and J. Dowling, editors. Harvard, Cambridge

Slayman, C.L., Long, W.S., Gradmann, D. 1976. "Action potentials" in *Neurospora crassa*, a mycelial fungus. *Biochim. Biophys. Acta* **426:**732–744

Spalding, E.P., Slayman, C.L., Goldsmith, M.H.M., Gradmann, D., Bertl, A. 1992. Ion channels in *Arabidopsis* plasma membrane: Transport characteristics and involvement in light-induced voltage changes. *Plant Physiol.* **99:**96–102

Tanifuji, M., Sato, M., Wada, Y., Anraku, Y., Kasai, M. 1988. Gating behaviors of a voltage-dependent and Ca^{2+}-activated cation channel of yeast vacuolar membrane incorporated into planar lipid bilayer. *J. Membrane Biol.* **106:**47–55

Tester, M., 1990. Plant ion channels: whole-cell and single-channel studies. *New Phytol.* **114:**305–340

Van de Mortel, J.B.J., Mulders, D., Korthout, H., Theuvenet, A.P.R., Borst-Pauwels, G.W.F.H. 1988. Transient hyperpolarization of yeast by glucose and ethanol. *Biochim. Biophys. Acta* **936:**421–428

Vergara, C., Latorre, R. 1983. Kinetics of Ca^{2+}-activated K^+ channels from rabbit muscle incorporated into planar bilayers. *J. Gen. Physiol.* **82:**543–568

Wada, Y., Ohsumi, Y., Tanifugi, M., Kasai, M., Anraku, Y. 1987. Vacuolar ion channel of the yeast, *Saccharomyces cerevisiae*. *J. Biol. Chem.* **262:**17260–17263

Yellen, G., 1984. Ionic permeation and blockade in Ca^{2+}-activated K^+ channels of bovine chromaffin cells. *J. Gen. Physiol.* **84:**157–186

Yellen, G. 1987. Permeation in potassium channels: Implications for channel structure. *Annu. Rev. Biophys. Biophys. Chem.* **16:**227–246

Zhou, X.-L., Stumpf, M.A., Hoch, H.C., Kung, C. 1991. A mechanosensitive channel in whole cells and in membrane patches of the fungus *Uromyces*. *Science* **253:**1415–1417

Received 9 July 1992; revised 18 November 1992